Supplement of The Airborne ROmanian Measurements of Aerosols and Trace gases (AROMAT) campaigns

Alexis Merlaud[1], Livio Belegante[2], Daniel-Eduard Constantin[3], Mirjam Den Hoed[4], Andreas Carlos Meier[5], Michel Van Roozendael[1], Marc Allaart[4], Maxim Arseni[3], Magdalena Ardelean[6], Tim Bösch[5], Hugues Brenot[1], Andreea Calcan[6], Emmanuel Dekemper[1], Sebastian Donner[8], Steffen Dörner[8], Lucian Georgescu[3], Anca Nemuc[2], Doina Nicolae[2], Reza Shaiganfar[8], Jeni Vasilescu[2], Andreas Richter[5], Adrian Rosu[3], Thomas Ruhtz[7], Anja Schönardt[5], Dirk Schuettemeyer[10], Kerstin Stebel[9], Frederik Tack[1], Sorin Nicolae Vâjâiac[6], Jurgen Vanhamel[1], and Thomas Wagner[8]

[1]Royal Belgian Institute for Space Aeronomie (BIRA-IASB), Avenue Circulaire 3, 1180 Brussels, Belgium
[2]National Institute of R&D for Optoelectronics (INOE), Magurele, Street Atomistilor 409, Magurele 77125, Romania
[3]"Dunarea de Jos" University of Galati, Faculty of Sciences and Environment, Str. Domneasca, Nr. 111, Galati 800008, Romania
[4]Royal Netherlands Meteorological Institute (KNMI), De Bilt, The Netherlands
[5]Institute of Environmental Physics, University of Bremen, Otto-Hahn-Allee 1, 28359 Bremen, Germany
[6]National Institute for Aerospace Research "Elie Carafoli" (INCAS), Bd. Iuliu Maniu no. 220, Bucharest, Romania
[7]Institute for Space Sciences, Free University of Berlin, Carl-Heinrich-Becker-Weg 6-10, 12165 Berlin, Germany
[8]Max-Planck-Institute for Chemistry (MPIC), Hahn-Meitner-Weg 1, 55128 Mainz, Germany
[9]Norwegian Institute for Air Research (NILU), Instituttveien 18, 2007 Kjeller, Norway
[10]European Space Agency (ESA-ESTEC), Keplerlaan 1, 2201 AZ Noordwijk, The Netherlands

Correspondence: A.Merlaud (alexism@oma.be)

1 Main instruments operated during the AROMAT campaigns

1.1 Airborne remote sensing

1.1.1 AirMAP

The AirMAP (Schönhardt et al., 2015; Meier et al., 2017) has been developed at IUP-Bremen. It is a pushbroom UV/vis imager
5 with a field-of-view of around $51°$, leading to a swath width of about the flight altitude. Light is collected by optical fibers from 35 individual viewing directions. The spectrometer is an Acton 300i imaging spectrograph with a focal length of 300 mm, and a f-number of f/3.9. When measuring primarily NO_2, AirMAP records spectra in the range 420-461 nm (AROMAT-1 settings) or 429-493 nm (AROMAT-2 settings). For the SO_2 measurements, the spectral range was set to 303-367 nm. For this UV configuration, the field-of-view decreases to $44°$. The spectrometer is temperature stabilized at 35 °C. AirMAP was installed
10 in the FUB Cessna during the AROMAT campaigns.

1.1.2 SWING

The SWING payload has been developed at BIRA-IASB. It is a compact whiskbroom UV/vis imager. SWING was upgraded between AROMAT-1 and AROMAT-2. Merlaud et al. (2018) describes the instrument used in AROMAT-1. For AROMAT-2, the instrument capabilities in the UV were improved, which enabled to simultaneously measure SO_2 and NO_2. Light is collected by a scanning mirror driven by a micocontroller. The spectrometer is an Avantes spectrometer (ULS-2048XL) with a focal length of 75 mm, which covers the spectral range of 280-550 nm. The field-of-view of the instrument is tunable but can reach 100°. The instantaneous field-of-view is 5°. The SWING instrument is 12 cm x 8 cm x 33 cm large and weight 1.2 kg. SWING was operated from the UGAL UAV during AROMAT-1 and from the FUB Cessna during AROMAT-2.

1.1.3 ULM-DOAS

The ULM-DOAS payload Constantin et al. (2017) is based on an ULS-2048XL Avantes spectrometer with a focal length of 75 mm, which covers the spectral range of 280-550 nm. A piece of wood under the aircraft wing holds the telescope, which has a 1.2 °field-of-view in the nadir direction. Light is sent from this input optics to the spectrometer by an optical fiber of 400 μ m. A laptop controls the acquisition and stores the spectra as well as the georeferencing data of a GPS antenna. The entire set-up is powered by the 12 V of the aircraft through an inverter. The ULM-DOAS measured NO_2 and SO_2 from the UGAL ultralight aircraft above the Jiu Valley during the AROMAT-2 campaign.

1.1.4 IUP-Bremen nadir-only DOAS

A nadir-only DOAS system was operated alongside AirMAP during AROMAT-2. The spectrometer is an Avantes ULS 2048x64, it has a focal length of 75 mm and covers the spectral range 287-551 nm at a spectral resolution of 0.8 nm (FWHM). A round-to-linear bundle of 14 100 μm thick fibers collects the light, achieving an effective field of view of 8.1°. This leads to an across track footprint of 425 m at 3 km a.g.l. During the Bucharest flight for H_2CO, the integration time was set to 30 s which leads to a pixel length of 1.8 km.

1.1.5 FUBISS-ASA2

The airborne spectrometer system FUBISS-ASA2 (Zieger et al., 2007) has been developed at the Institute for Space Sciences at the Free University of Berlin. It simultaneously measures the direct solar irradiance and the aureole radiance in two different solid angles. Light is collected by a sun tracker. Ring shaped apertures shield the direct sunlight and only allow radiation between 4°and 6°. The spectrometers used for the sun as well as the aureole photometers provide 256 evenly spaced channels from 300 to 1000 nm. During the AROMAT campaigns, the FUBISS-ASA2 was operated from the FUB Cessna and provided aerosol optical depth profiles in the vicinity of Bucharest.

1.2 Airborne in-situ

1.2.1 KNMI NO_2 sonde

The measurement principle of the KNMI NO_2-sonde(Sluis et al., 2010) is based upon the chemical reaction between NO_2 and luminol, a chemiluminescent reaction that produces a faint blue light. Ambient air is pumped through a teflon pump, and bubbled through the sensing solution. The light that is produced by the reaction is detected by an array of photodiodes that is glued to the reaction chamber. The electric current from the photodiodes is converted into a voltage with a highly sensitive operational amplifier, and passed through a filter that removes high frequency fluctuations. During AROMAT-1, the NO_2-sonde was mounted on the UGAL UAV and attached to meteorological balloons. During AROMAT-2, the NO_2-sonde was installed onboard the INCAS BN-2.

1.2.2 AS32M CAPS

The AS32M NO_2 monitor is a commercial instrument manufactured by Environnement S.A. It follows the Cavity Attenuated Phase Shift (CAPS) principle(Kebabian et al., 2005). It measures the NO_2 volume mixing ratio using a blue light-emitting diode (LED) as a light source, a near-co focal arrangement of two high reflectivity mirrors in tandem with an enclosed sample cell of 26 centimeter in length and a vacuum phototube detector. The wavelength and spectral band pass of the measurement are defined by the use of an interference filter centered at 450 ± 10 nanometer. The monitor is enclosed within a standard 19 inch rack-mounted instrumentation box, weighs 12.5 kilogram, and uses 225 Watts of electrical power including the vacuum pump. The NO_2 CAPS was mounted onboard the BN-2 during AROMAT-2.

1.2.3 TSI Aerodynamic particle sizer

The TSI Aerodynamic Particle Sizer 3321 (Pfeifer et al., 2016) provides the diameter of particles in the range 0.5-20 μm. Particles are accelerated on an air flow through a nozzle and their times of flight measured between two lasers provide proxies for their sizes. During AROMAT-1, this instrument was mounted on the INCAS UAV. During AROMAT-2 it was installed in the INCAS BN-2.

1.2.4 PICARRO G2401-mc

The Picarro G2401-mc is a commercial instrument that simultaneously quantifies the concentrations of water vapor, carbon monoxide, carbon dioxide and methane(Chen et al., 2013). The instrument uses a tunable laser and applies the cavity ring down spectroscopy technique to measure spectral absorption of molecules in an optical cavity. The model G2401-mc is designed for airborne operations and also provides the dry gas mole fractions. The PICARRO G2401-mc was operated from the BN-2 during AROMAT-2.

1.3 Car-based Mobile-DOAS systems

1.3.1 BIRA Double channel Mobile-DOAS

The BIRA double channel Mobile-DOAS instrument(Merlaud, 2013) is based on a double channel Avantes spectrometer installed on a car. The entry slit is 50 μm, the focal length 75 mm and the grating is a 600 l.mm^{-1}, blazed at 300 nm. The spectral range is 200-750 nm with a 1.3 nm resolution (FWHM). The CCD detector is a Sony2048 linear array with a Deep-UV coating for signal enhancement below 350 nm. An optical head, mounted on the car window, holds the two telescopes achieving a 2.5 °field-of-view with fused silica collimating lenses. One telescope points zenith while the other is directed 30°above the horizon. Two 400 μm chrome plated brass optical fibers connects the telescopes to the spectrometer. The integration time is around 5ms. Each measurement is an average of (typically) 10 seconds of 10 scans accumulations. A GPS antenna is used for georeferencing the measurement, the whole set-up is powered by the car 12V through an inverter. While measuring, the instrument is recording spectra continuously and simultaneously from the two directions.

1.3.2 UGAL and BIRA zenith-only Mobile-DOAS

The zenith only Mobile DOAS systems used by UGAL and BIRA(Constantin et al., 2013) are based on Avantes spectrometers installed on a car. They have only one zenith channel, the entry slit is 50 μm, the focal length 75 mm and the grating is a 1200 l.mm^{-1}, blazed at 250 nm. The spectral range is 290-550 nm with a 0.7 nm resolution (FWHM). The CCD detector is a 2048 linear array Hamamatsu S11155 with pixels of 14 μm x 500 μm. The fiber is attached to the car and points to the zenith through a fused silica collimating lens resulting in a field of view of 2.5 °. The integration time is around 150ms. Each measurement is an average of (typically) 10 seconds of 10 scans accumulations. The system also uses a GPS antenna for georeferencing the measurements and is also powered by an inverter plugged on the car 12V.

1.3.3 MPIC Scanning Mobile-DOAS

Two mobile Max-DOAS instruments were used by MPIC during the AROMAT campaigns: a Mini-MAX-DOAS and a newly developed instrument, the so-called Tube MAX-DOAS.

The Mini-MAX-DOAS instrument is a commercial instrument produced by Hoffman GMBH, it is described in detail by (Wagner et al., 2010) which also presents its car-based operation. This instrument uses a thermoelectrically cooled USB2000+ Ocean Optics spectrometer. The latter covers the spectral range 320-460 nm at a spectral resolution of 0.7 nm. Light is collected within a field of view of 1.2°through a lens of focal length 40 mm. The optics, spectrometer, and controlling electronics is mounted in a sealed-box enclosure. The whole set-up is rotated by a stepper motor.

The Tube MAX-DOAS has been developed at MPIC and is based on an ULS 2048x64 Avantes spectrometer which covers the spectral range 315-474 nm at a spectral resolution of 0.7 nm FWHM. This spectrometer uses a 100 μm entry slit, a 1800 l.mm^{-1} grating, and a Schott BG3 filter to reduce the visible straylight. The spectrometer is installed inside the car and stabilized at 15°C. It is connected to the telescope unit through a round-to-linear fibre bundle based on 4 monofibers of

diameter 200 μm. The telescope unit consists of a stepper motor inside a plastic tube which rotates the fiber and a 50 mm lens outside the tube, leading to a field of view of about 0.7°.

1.4 Ground-based remote sensing

1.4.1 INOE RALI lidar

The Multiwavelength depolarization Raman Lidar RALI (Nicolae et al., 2010; Belegante et al., 2011) measures the Raman backscattering radiation from atmospheric water vapor, nitrogen, and Mie/Rayleigh backscattering radiation from atmospheric molecules and aerosol particles. It emits and receives light at 1064, 532, and 355 nm. The output parameters are the backscatter coefficient, the extinction coefficient, water vapor mixing ratio, and particle depolarization ratio. The altitude of full overlap is around 800 m. Advanced products have been dedicated to aerosol typing (Nicolae et al., 2018), microphysical inversion and aerosol mass concentration retrievals. The system is part of the European Aerosol Research Lidar Network (EARLINET) as an advanced Lidar station. This instrument performed measurements during both of the campaigns only in Magurele at RADO observatory.

1.4.2 INOE MILI lidar

The UV depolarization eye-safe Lidar MILI detects Mie/Rayleigh backscattering from atmospheric molecules and aerosol particles. It emits laser pulses at 355 nm (20mJ) and measures the backscattered light in two orthogonal polarization states. The laser pulse duration is 8 ns (at 355 nm), the repetition rate is 20Hz, and the beam diameter lies between 3 and 5 mm (FWHM). The dynamic range covers 1-5 km, depending on the atmosphere transmission, with a spatial resolution of 7.5 m. The reception uses a 200 mm Cassegrain telescope, and the system acquisition is analog and photon counting, with 20 MS.s^{-1} analog sampling rate and 250 MHz photon counting count rate. The altitude of full overlap was around 500 m during the AROMAT campaigns, it can be aligned to 300 m.

1.4.3 SO$_2$ camera

The SO$_2$ camera is an updated version of the Envicam-2 system described in Kern et al. (2015). It uses a Hamamatsu C8484 fast-sampling camera (1344x1024 pixels), a four-position filter wheel, and a UV spectrometer. The filter wheel holds two 10 nm filters centered at 310 and 325 nm, respectively corresponding to a strong and weak absorption of SO$_2$, a UV broadband view, and a blackened plate for dark-current measurements. A co-aligned spectrometer receives light within a field-of-view of 0.33°through a 100 mm diameter lens. During AROMAT-2, we used a 25 mm lens for the camera, leading to a field of view of 14.3°x 10.9°.

1.5 ALTIUS NO$_2$ camera

The NO$_2$ camera is a hyperspectral imager that can take spectral images of a scene with a spectral resolution better than 1 nm (Dekemper et al., 2016). The tuning of the acquisition wavelength is sequential, but takes place in a few milliseconds.

The passband selection is made by an acousto-optical tunable filter (AOTF). The AOTF principle relies on the acousto-optic interaction in a birefringent crystal: the passband central wavelength is determined by the frequency of an acoustic wave propagating in the crystal. Its main advantages are: a small and lightweight packaging, a low power consumption, a fast response, and a high diffraction efficiency. This instrument is composed of a telecentric optical system which images a scene with a 6°x 6° square field of view (FOV) onto a CCD camera (512x512 pixels). In typical light conditions, a frame rate of 1 Hz is achieved. Thanks to its imaging capabilities, and its frame rate, this instrument is capable of tracking the signature of NO_2 in dynamic targets, such as smokestacks exhausts.

1.6 Ground-based in-situ

1.6.1 Aerosol mass spectrometer

The compact time-of-flight aerosol mass spectrometer (AMS) measures the chemical composition and size resolved mass concentration of non-refractory PM1 aerosols, using mass spectrum or particle time-of-flight mode of operation (Jayne et al., 2000). The AMS samples continuously aerosols near to the ground through a 100 μm critical orifice. The particles are thermal vaporized, followed by the electron impact ionization of the vaporized species and detection by mass spectrometry. The output parameters are mass concentration time series for organics, nitrate, sulfate, ammonium, chloride aerosols species and vacuum aerodynamic size distribution of submicronic aerosols.

1.6.2 Aerosol Chemical Speciation Monitor

Aerosol Chemical Speciation Monitor (ACSM) is a simplified version of the AMS, using a quadrupole mass spectrometer (Petit et al., 2015). An automated zeroing system is implemented, which measure alternatively particle-free sample or ambient particles using the filter and sample mode of operation. Also a naphthalene filter is used as an internal calibration standard. The output parameters are average mass concentrations of particulate organics, sulfate, nitrate, ammonium and chloride.

Table S1. Typical air mass factors (AMF), 1-σ DOAS fitting errors (σ_S), and integration times (Tint) for the NO_2 DOAS instruments.

	AMF	σ_S (molec cm^{-2})	Tint
AirMAP	1.5	2.2x10^{15}	0.5 s
SWING	1.5	1.8x10^{15}	0.5 s
ULM-DOAS	1.5	8x10^{14}	10 s
Tube MAX-DOAS	2	2.5x10^{14}	30 s
Mini MAX-DOAS	2	1.2x10^{15}	30 s
UGAL Mobile-DOAS	1	4x10^{14}	30 s
BIRA Mobile-DOAS	1	8x10^{14}	30 s

Table S2. Typical air mass factors (AMF), 1-σ DOAS fitting errors (σ_S), and integration times (Tint) for the SO_2 DOAS instruments.

	AMF	σ_S (molec cm^{-2})	Tint
AirMAP	1	1.7×10^{16}	0.5 s
SWING	1	2×10^{16}	0.5 s
ULM-DOAS	1	5×10^{15}	10 s
Tube MAX-DOAS	2	1×10^{16}	30 s
Mini MAX-DOAS	2	2×10^{16}	30 s
UGAL Mobile-DOAS	1	4×10^{15}	30 s

Table S3. Typical air mass factors (AMF), 1-σ DOAS fitting errors (σ_S), and integration times (Tint) for the H_2CO DOAS instruments.

	AMF	σ_S (molec cm^{-2})	Tint
Bremen nadir	1	6×10^{15}	30 s
Tube MAX-DOAS	2	1.6×10^{15}	30 s

2 Practical implementations of the campaigns

2.1 The 2014 AROMAT campaign

150 The AROMAT-1 campaign took place between 1 and 13 September 2014. The operations started in Bucharest with the continuous observations from the Romanian Atmospheric 3D Observatory (RADO, Nicolae et al. (2010)) observatory and synchronized car-based Mobile-DOAS observations around the Bucharest ring road and within the city. During the first two days of the campaign, the INCAS UAV flew from the Clinceni airfield with two different aerosol payloads (the TSI Dust Trak DRX and TSI aerosol particle sizer) up to an altitude of 1.2 km a.s.l. The Cessna was not allowed to fly over the city but performed

155 loops above the ring road at a low altitude of 500 m a.s.l. The remote sensing measurements stopped on 4 September due to bad weather. On 5 and 6 September, we collected data only from the ground, and in broken cloud conditions.

On 7 September 2014, part of the campaign crew moved to the Jiu Valley. We installed the INOE mobile laboratory (in-situ monitors, MILI lidar, and ACSM) in Turceni and performed the first UAV flights around the power plant on 8 September 2014 with the NO_2 sonde and SWING. On the same day in Bucharest, the Cessna flew above the city with AirMAP and Mobile-

160 DOAS operated on the ground. On the following day, 9 September 2014, the Cessna did a second mapping of Bucharest and we started to launch balloons from Turceni, carrying the NO_2 sonde. In total, 11 balloons were launched between 8 and 12 September 2014, out of which 10 led to successful measurements. Technical issues with both the UAV and the Cessna interrupted the flights for a couple of days. The UAV operations started again with a SWING flight on 10 September 2014. On 11 September 2014, the AirMAP and SWING flew in coincidence above Turceni, on the Cessna and the UAV respectively, and

165 we performed two more short SWING-UAV flights. On 12 and 13 September, we performed two more Cessna flights above the Jiu Valley but the weather conditions were degrading. During the entire second week of the campaign, Mobile-DOAS measurements were performed in Turceni and around the other power plants of the Jiu Valley.

Table S4 summarizes the main measurement days during AROMAT-1, specifying if the measurements were taken in Bucharest or in the Jiu Valley. The "golden days" of the AROMAT-1 campaigns are 2, 8, and 11 September 2014. These days are particularly interesting due to good weather conditions and coincident measurements. On 2 September 2014, we operated the three Mobile-DOAS together around Bucharest. On 8 September 2014, we flew AirMAP above Bucharest with the UGAL and MPIC Mobile-DOAS on the ground. Finally, on 11 September 2014, SWING and AirMAP were time-coincident above the Turceni power plant, and two balloons sampled the vertical distribution of NO_2.

Table S4. Measurements table during the AROMAT 2O14 campaign. B stands for Bucharest, J for the Jiu Valley.

	1-9-14	2-9-14	3-9-14	7-9-14	8-9-14	9-9-14	11-9-14	12-9-14
AirMAP	B	B	-	-	B	B	J	J
SWING	-	-	-	-	-	J	J	-
NO_2 sonde	-	-	-	-	J	J	J	J
APSR	B	B	-	-	-	-	-	-
BIRA Mobile-DOAS	B	B	B	J	J	J	J	J
UGAL Mobile-DOAS	B	B	B	B	B	J	J	J
MPIC Mobile-DOAS	-	B	B	B	B	J	J	J
RALI	B	B	-	B	B	B	B	B
MILI	B	B	-	-	-	J	J	-
ACSM	B	B	B	-	J	J	J	-
AMS	B	B	B	B	B	B	B	B
Trace gas monitors	B	B	B	-	J	J	J	-

2.2 The 2015 AROMAT-2 campaign

The AROMAT-2 campaign took place between 17 and 31 August 2015. We started in Bucharest with car-based Mobile-DOAS measurements and observations at RADO. The INOE mobile lab was installed in Turceni on 19 August 2015, followed by the SO_2 (Kern et al., 2015; Stebel et al., 2015) and NO_2 camera Dekemper et al. (2016). Poor weather conditions limited the relevance of the measurements during the first days of the campaign. Two Mobile-DOAS teams in Bucharest moved from Bucharest to the Jiu Valley on 23 August 2015. From then, the weather was fine until the end of the campaigns, and valuable data were collected during all days between 24 and 31 August 2015.

In the Jiu Valley, the crew was based in Turceni and most of the static instruments were installed at a soccer field. Beside the INOE mobile lab with in-situ samplers, the scanning lidar, SO_2 cameras and the NO_2 camera pointed to the power plant plume. The NO_2 camera acquired images until 25 August 2015. The car-based Mobile-DOAS operated in the Valley between the different power plants. From 24 August, the SO_2 cameras were splitted: one of them stayed in the soccer field, the two others were installed at several points around Turceni. Also on 24 August, the UGAL ultralight took off from Craiova and flew

to the Jiu Valley until Rovinari, carrying a nadir-looking spectrometer. This experiment was repeated on 25, 26, and 27 August. On 28 August 2015, the Cessna flew above Turceni with AirMAP and SWING.

In Bucharest, the BN-2 flew first on 25 August 2015. It took off from Strejnicu and carried various in-situ instruments: the TSI nephelometer and Aerosol Particle Sizer, the NO_2 CAPS, the PICARRO, and the KNMI NO_2 sonde, and flew in a loop pattern at 500 m a.s.l. around the city ring road. After this test flight, the aircraft performed 6 flights between 27 and 31 August 2015, which included soundings around Baneasa and Magurele, up to 3300 m a.s.l. On 30 and 31 August 2015, the Cessna mapped the city of Bucharest, performing two flights per day. It also performed soundings to measure AOD profiles with the FUBISS-ASA2 instrument (Zieger et al., 2007).

Table S5 summarizes the measurements of the AROMAT-2 campaign, specifying if the measurements were taken in Bucharest or in the Jiu Valley. Compared to the AROMAT-1 campaign, a larger number of instruments took part and also a larger number of 'golden days' occurred. All the days between 24 and 31 August 2015 led to interesting measurements. Regarding intercomparison exercises for the airborne imagers, the best days are 28 August 2015 (Jiu Valley) and 31 August 2015 (Bucharest).

Table S5. Measurements during the AROMAT 2O15 campaign. B stands for Bucharest, J for the Jiu Valley.

	24-8-15	25-8-15	26-8-15	27-8-15	28-8-15	29-8-15	30-8-15	31-8-15
AirMAP	-	-	-	-	J	-	B	B
SWING	-	-	-	-	J	-	B	B
FUBISS	-	-	-	-	-	-	B	B
ULT-DOAS	J	J	J	J	-	-	-	-
NO_2 camera	J	J	-	-	-	-	-	-
SO_2 camera	J	J	J	J	J	J	-	-
NO_2Sonde	-	B	-	B	B	-	-	-
CAPS	-	B	-	B	B	-	B	B
Nephelometer	-	B	-	B	B	-	B	B
PICARRO	-	B	-	B	B	-	B	B
APSR	-	B	-	B	B	-	B	B
BIRA Mobile-DOAS	J	J	J	J	J	B	B	B
MPIC Mobile-DOAS	J	J	J	J	J	B	B	B
UGAL Mobile-DOAS	-	-	-	J	J	B	B	B
RALI	B	B	B	B	B	B	B	B
MILI	J	J	J	J	J	J	-	-
ACSM	B	B	B	-	J	J	J	-
AMS	B	B	B	B	B	B	B	B
Trace gas monitors	J	J	J	J	J	J	-	-

3 Intercomparison results
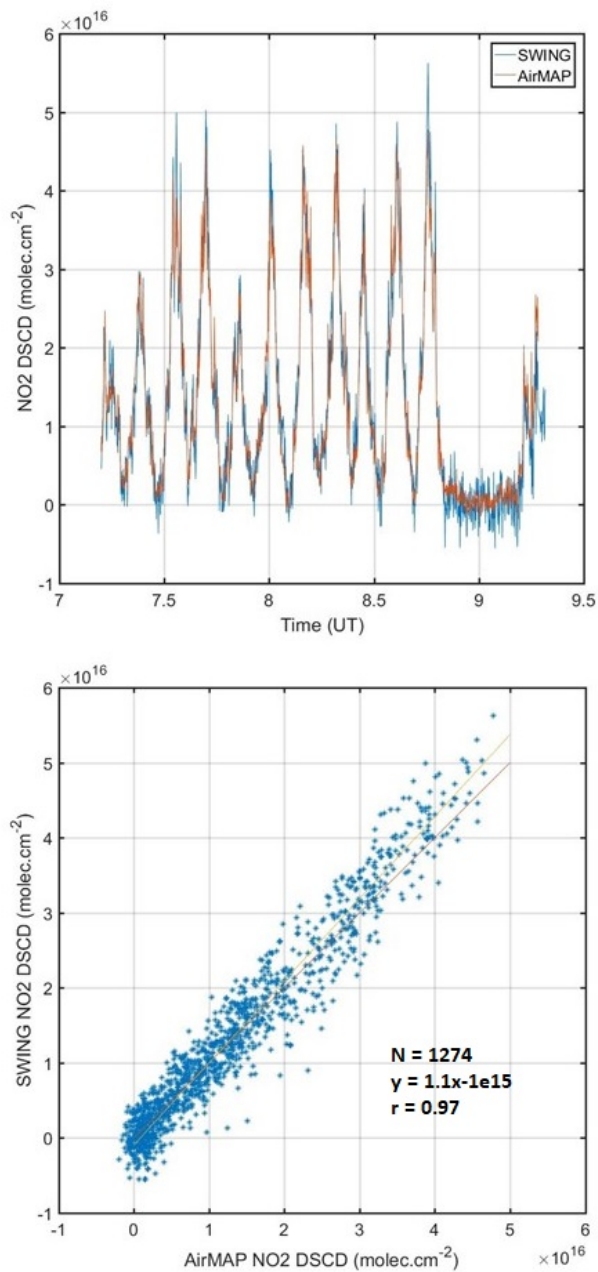
Figure S1. Comparison of the AirMAP and SWING NO₂ DSCDs above Bucharest (31 August 2015). The lower panel also shows the orthogonal regression (blue) and 1:1 (red) lines.
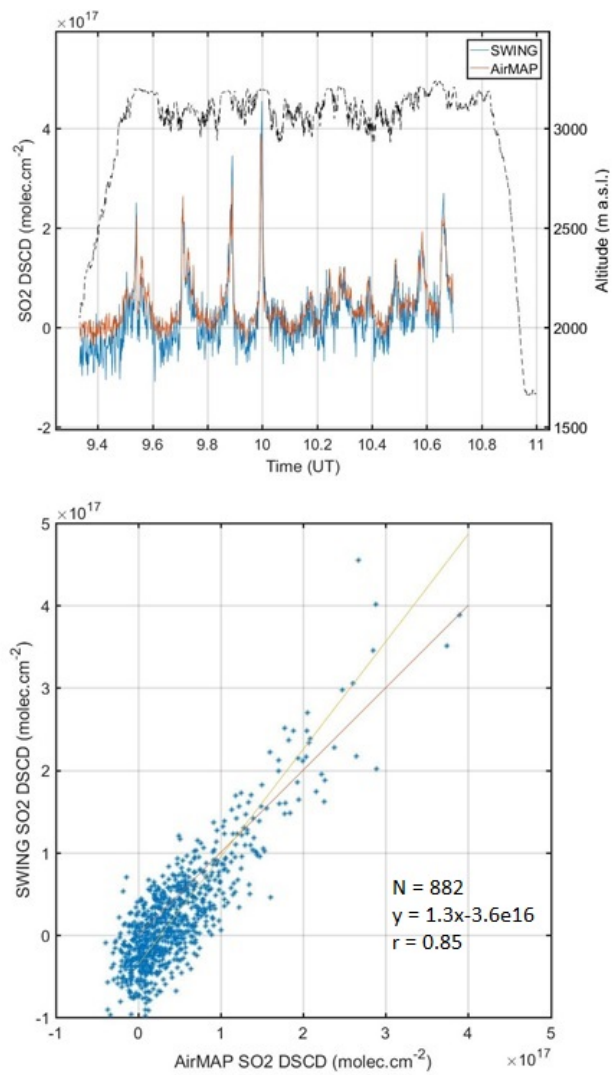
Figure S2. Comparison of the AirMAP and SWING SO$_2$ DSCDs above the Jiu Valley (28 August 2015). The upper panel also shows the flight altitude. The lower panel shows the orthogonal regression (blue) and 1:1 (red) lines.
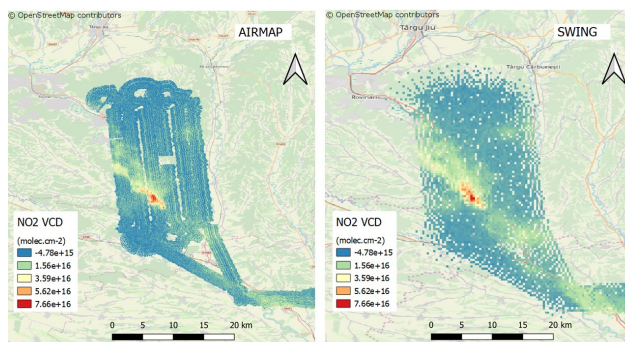
Figure S3. AirMAP (left panel) and SWING (right panel) NO$_2$ VCDs above Turceni (28 August 2015).
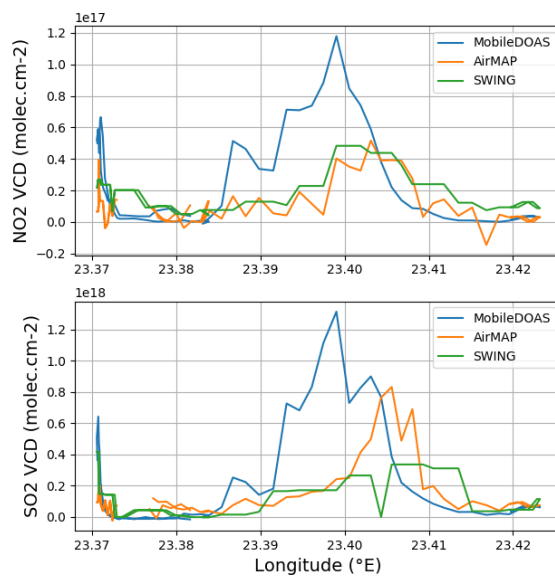
Figure S4. Comparison of the AirMAP, SWING, and Mobile DOAS SO$_2$ and NO$_2$ VCDs around Turceni Jiu (28 August 2015)
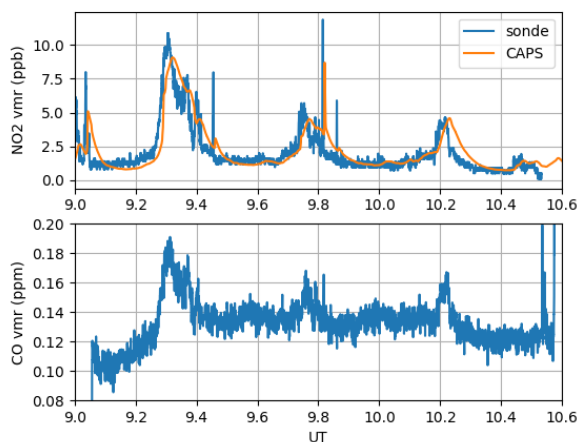
Figure S5. CAPS (orange) and NO_2 sonde (blue) measurements (upper panel) with CO measurements from the PICARRO (lower panel) onboard the BN-2 around Bucharest (25 August 2015). Note that the longer response time of the CAPS explains its time shift compared to the sonde.
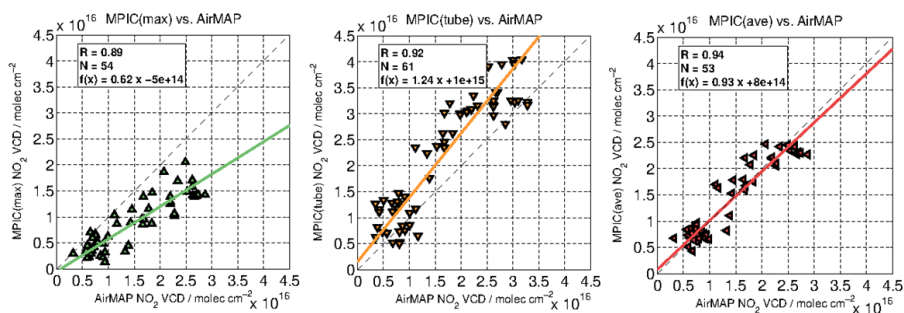
Figure S6. Comparison of AirMAP and MPIC Mobile DOAS NO_2 VCDs measurements during the morning flight on 31 August 2015. The left panel compares AirMAP with the Mini-MAX-DOAS which pointed forward, 22° above the horizon. The middle panel compares AirMAP with the Tube MAX-DOAS which pointed backward, 22° above the horizon. The right panel compares AirMAP with the average of the Mini-MAX-DOAS and Tube MAX-DOAS.

4 Geophysical findings
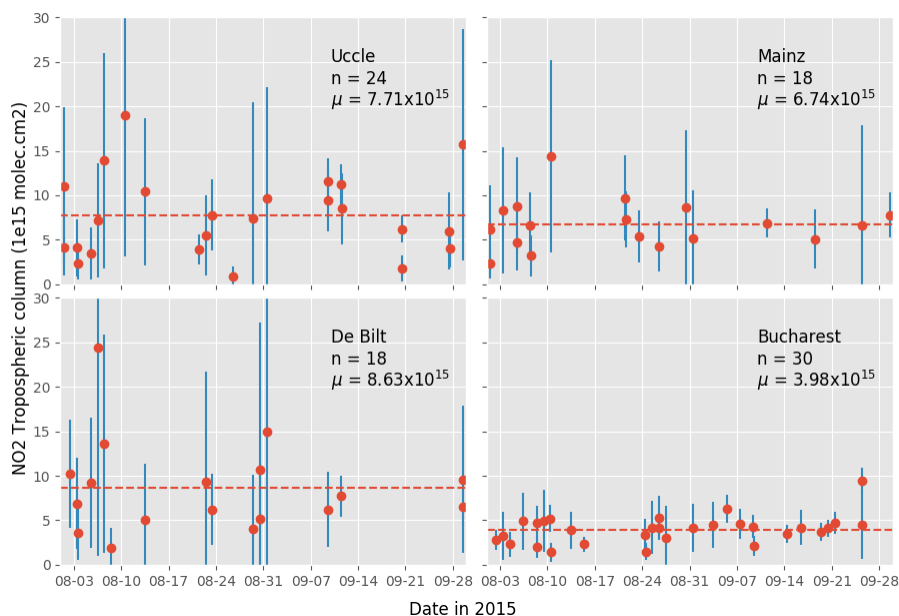
Figure S7. Tropospheric NO_2 VCDs for OMI overpasses around four European sites including Bucharest, filtered to remove cloudy scenes and row anomalies (TEMIS NO_2 overpass data). The red dashed line indicates the mean NO_2 VCD in the time window. The NO_2 column is smaller above Bucharest. This site is less affected by clouds.
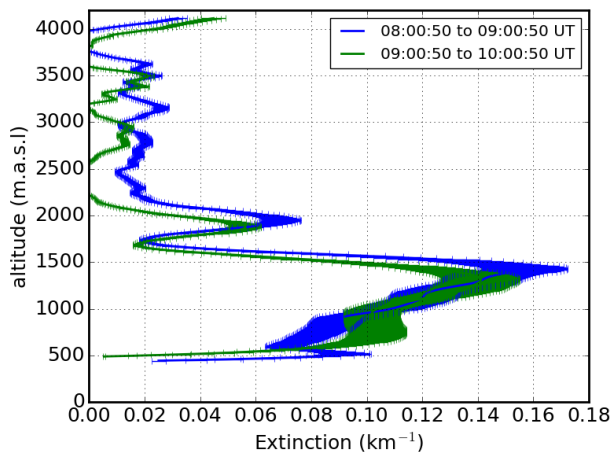
Figure S8. Extinction profiles measured in Turceni by the MILI lidar during the Cessna overpass on 28 August 2015. Note that the low values around 500 m are caused by the lidar partial overlap.
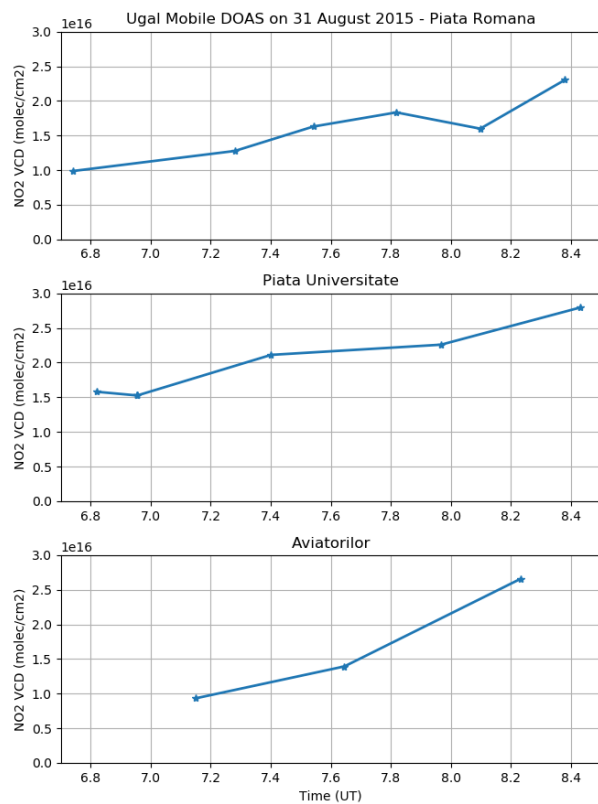
Figure S9. Time evolution of NO_2 VCDs measured with the mobile-DOAS measurements in the vicinity of three places of Bucharest on 31 August 2015.
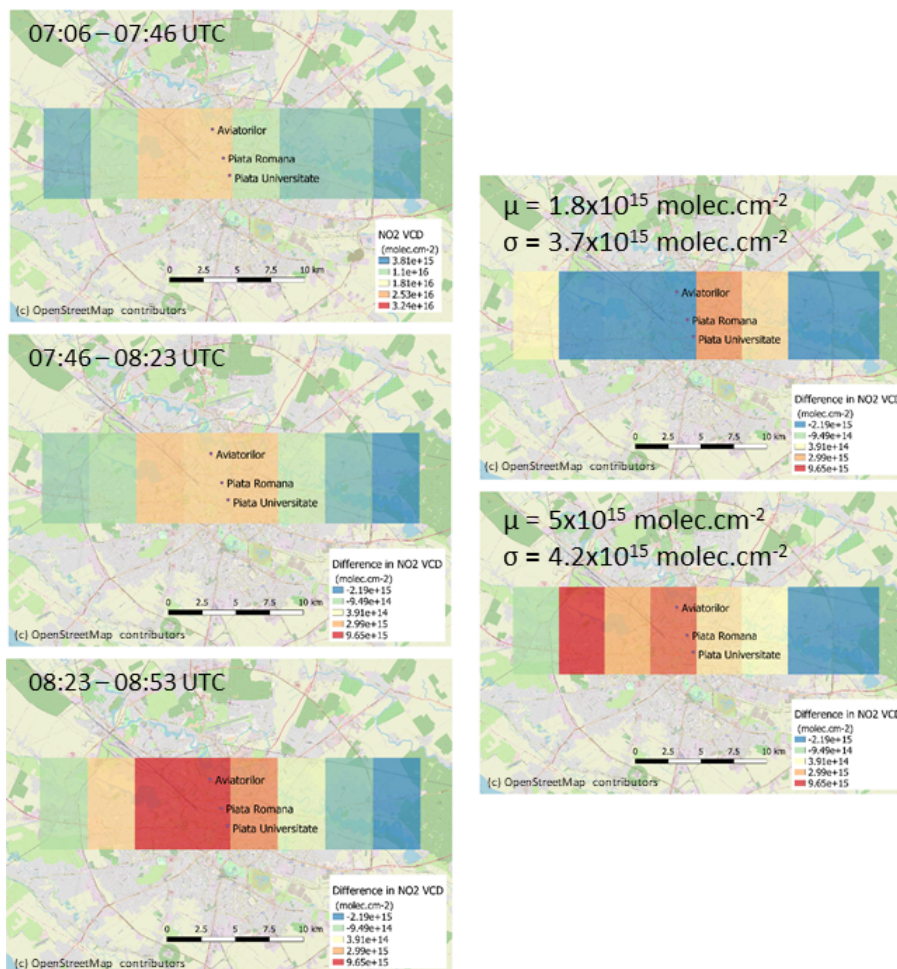
Figure S10. AirMAP measurements of NO$_2$ VCDs degraded at the TROPOMI resolution during three overpasses of the morning flight of 31 August 2015 (left panels), together with the differences of these degraded NO$_2$ VCDs for consecutive overpasses (right panels). The right panels also indicate the means (μ) and standard deviations (σ) of the two differences. The maps pinpoint the positions of the three mobile-DOAS sites of Fig.S9.
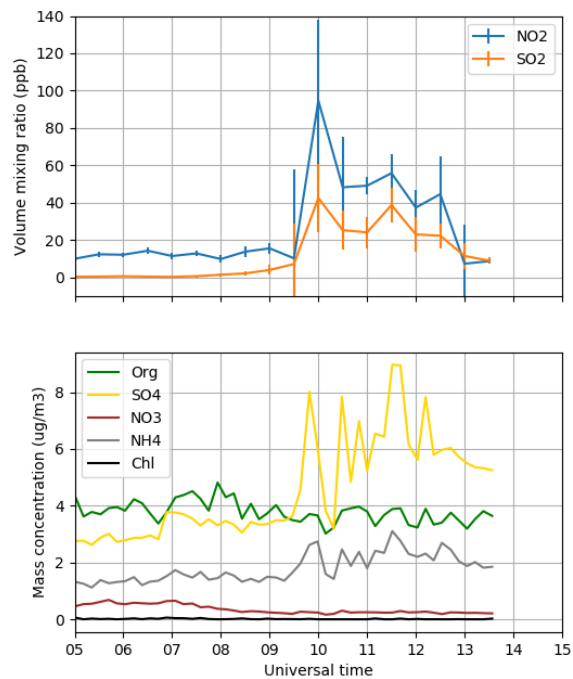
Figure S11. NO_2 and SO_2 in-situ and aerosol chemical speciation monitor measurements during AROMAT-1 (11 September 2014).
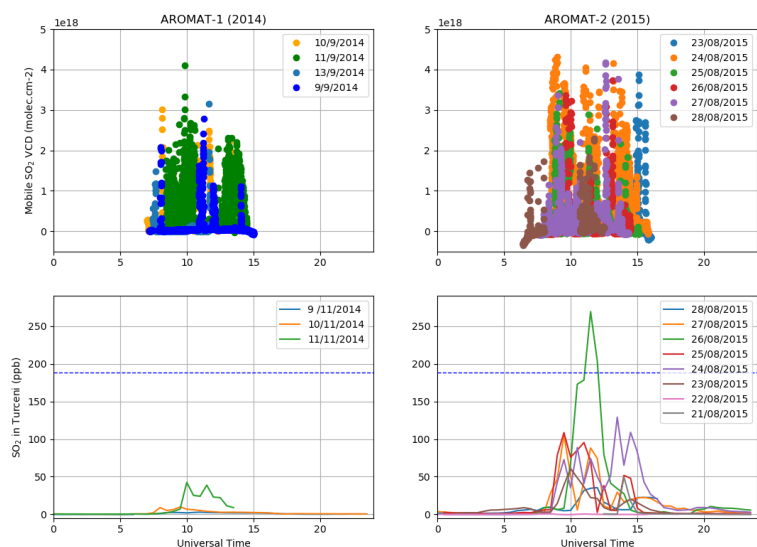
Figure S12. Zenith-only Mobile DOAS in the Jiu Valley and in-situ measurements in Turceni during AROMAT-1 (left panels) and AROMAT-2 (right panels). The blue dashed line indicates the 10 minutes mean threshold recommended by the World Health Organization.
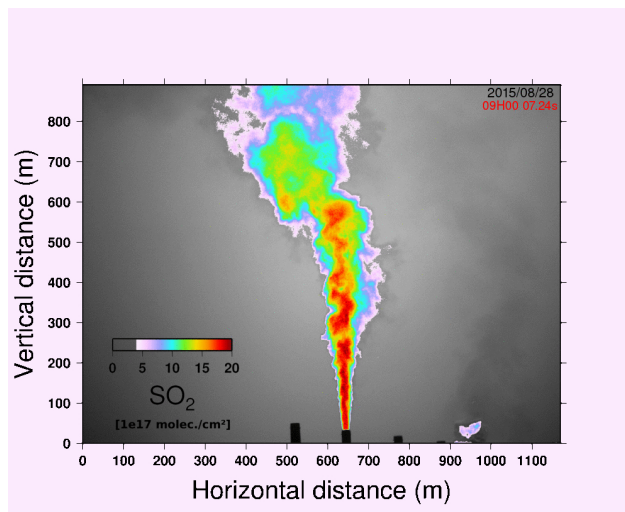
Figure S13. Image of the SO_2 plume above the Turceni power plant, recorded with the Envicam2 SO_2 camera (28 August 2015).
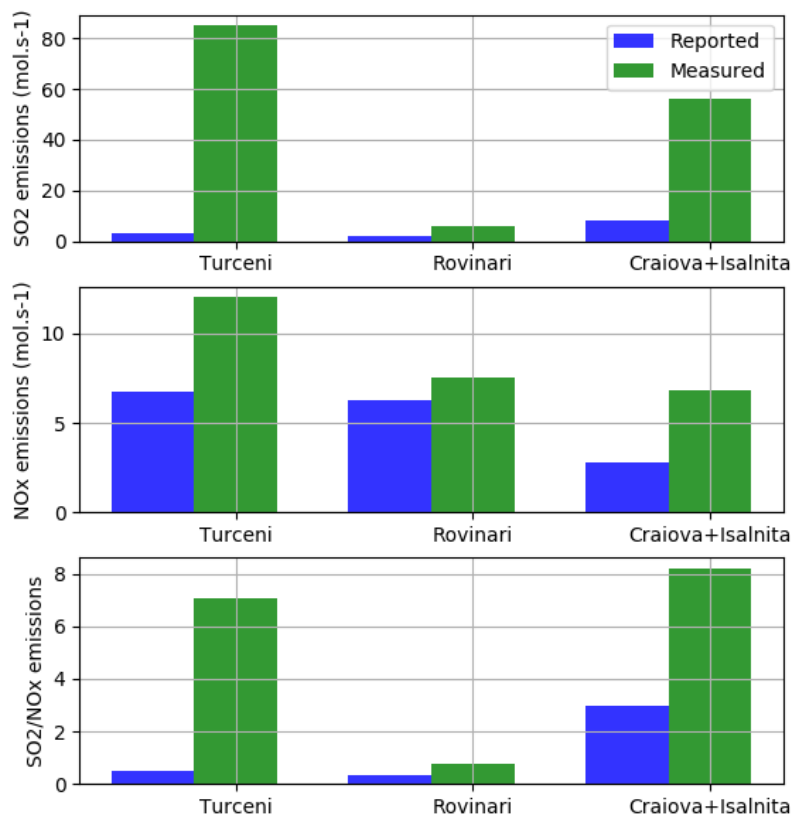
Figure S14. SO_2 and NO_x fluxes from the power plants of the Jiu Valley as (1) measured with the ULMDOAS measurements on 25 August 2015 (green bars) and (2) estimated from the reported emissions of 2015 assuming constant emissions (blue bars). Uncertainties on the ULMDOAS fluxes are around 60%.

Table S6. Range of measurements during the AROMAT 2014 campaign.

	Bucharest (min-max)	Jiu Valley (min-max)
NO vmr (ppb)	0-4	0-92
NO_2 vmr (ppb)	1-26	1-95
SO_2 vmr (ppb)	0-2	0-43
SO_2 column (molec.cm^{-2})	0-1e^{16}	0-4e^{18}
NO_2 column (molec.cm^{-2})	0-4e^{16}	0-1.3e^{17}
AOD (500 nm)	0.1-0.4	n.a
Aerosol extinction in BL (m^{-1})	6e^{-5} - 3.5e^{-4}	1e^{-4} - 2.8e^{-3}
Maximum boundary layer height (m)	2200	1500

Table S7. Range of measurements during the AROMAT 2015 campaign.

	Bucharest (min-max)	Jiu Valley (min-max)
CO vmr (ppm)	n/a	0.01-0.18
CH_4 vmr (ppm)	n/a	2.3-2.7
NO vmr (ppb)	n/a	0-18
NO_2 vmr (ppb)	n/a	1-34
O_3 vmr (ppb)	n/a	5-82
SO_2 vmr (ppb)	n/a	0-280
AOD (500 nm)	0.05-0.38	n/a
Aerosol extinction in BL (m^{-1})	1e^{-4} - 3e^{-4}	1e^{-4} - 4e^{-4}
Maximum boundary layer height (m)	3000	2300
SO_2 column (molec.cm^{-2})	n/a	0-4e^{18}
NO_2 column (molec.cm^{-2})	0-4e16	0-1.3e^{17}
H_2CO column (molec.cm^{-2})	1-7e^{16}	n/a

References

Belegante, L., Talianu, C., Nemuc, C., and Nicolae, D.: Detection of local weather events from multiwavelength lidar measurements during the EARLI09 campaign, Rom. J. Phys., 56, 484–494, 2011.

Chen, H., Karion, A., Rella, C. W., Winderlich, J., Gerbig, C., Filges, A., Newberger, T., Sweeney, C., and Tans, P. P.: Accurate measurements of carbon monoxide in humid air using the cavity ring-down spectroscopy (CRDS) technique, Atmos. Meas. Tech., 6, 1031–1040, https://doi.org/10.5194/amt-6-1031-2013, 2013.

Constantin, D., Merlaud, A., Van Roozendael, M., Voiculescu, M., Fayt, C., Hendrick, F., Pinardi, G., and Georgescu, L.: Measurements of Tropospheric NO2 in Romania Using a Zenith-Sky Mobile DOAS System and Comparisons with Satellite Observations, Sensors, 13, 3922–3940, https://doi.org/10.3390/s130303922, 2013.

Constantin, D.-E., Merlaud, A., Voiculescu, M., Dragomir, C., Georgescu, L., Hendrick, F., Pinardi, G., and Van Roozendael, M.: Mobile DOAS Observations of Tropospheric NO2 Using an UltraLight Trike and Flux Calculation, Atmosphere, 8, 78, https://doi.org/10.3390/atmos8040078, 2017.

Dekemper, E., Vanhamel, J., Van Opstal, B., and Fussen, D.: The AOTF-based NO2 camera, Atmos. Meas. Tech., 9, 6025–6034, https://doi.org/10.5194/amt-9-6025-2016, 2016.

Jayne, J. T., Leard, D. C., Zhang, X., Davidovits, P., Smith, K. A., Kolb, C. E., and Worsnop, D. R.: Development of an Aerosol Mass Spectrometer for Size and Composition Analysis of Submicron Particles, Aerosol Sci. Tech., 33, 49–70, https://doi.org/10.1080/027868200410840, 2000.

Kebabian, P. L., Herndon, S. C., and Freedman, A.: Detection of nitrogen dioxide by cavity attenuated phase shift spectroscopy, Anal. Chem., 77, 724–728, https://doi.org/10.1021/ac048715y, 2005.

Kern, C., Lübcke, P., Bobrowski, N., Campion, R., Mori, T., Smekens, J.-F., Stebel, K., Tamburello, G., Burton, M., Platt, U., and Prata, F.: Intercomparison of SO2 camera systems for imaging volcanic gas plumes, J. Volcanol. Geotherm. Res., 300, 22 – 36, https://doi.org/https://doi.org/10.1016/j.jvolgeores.2014.08.026, 2015.

Meier, A. C., Schönhardt, A., Bösch, T., Richter, A., Seyler, A., Ruhtz, T., Constantin, D.-E., Shaiganfar, R., Wagner, T., Merlaud, A., Van Roozendael, M., Belegante, L., Nicolae, D., Georgescu, L., and Burrows, J. P.: High-resolution airborne imaging DOAS measurements of NO$_2$ above Bucharest during AROMAT, Atmos. Meas. Tech., 10, 1831–1857, https://doi.org/10.5194/amt-10-1831-2017, 2017.

Merlaud, A.: Development and use of compact instruments for tropospheric investigations based on optical spectroscopy from mobile platforms, Presses univ. de Louvain, 2013.

Merlaud, A., Tack, F., Constantin, D., Georgescu, L., Maes, J., Fayt, C., Mingireanu, F., Schuettemeyer, D., Meier, A. C., Schönardt, A., Ruhtz, T., Bellegante, L., Nicolae, D., Den Hoed, M., Allaart, M., and Van Roozendael, M.: The Small Whiskbroom Imager for atmospheric compositioN monitorinG (SWING) and its operations from an unmanned aerial vehicle (UAV) during the AROMAT campaign, Atmos. Meas. Tech., 11, 551–567, https://doi.org/10.5194/amt-11-551-2018, 2018.

Nicolae, D., Vasilescu, J., Carstea, E., Stebel, K., and Prata, F.: Romanian Atmospheric research 3D Observatory: Synergy of instruments, Rom. Rep. Phys., 62, 2010.

Nicolae, D., Vasilescu, J., Talianu, C., Binietoglou, I., Nicolae, V., Andrei, S., and Antonescu, B.: A neural network aerosol-typing algorithm based on lidar data, Atmos. Chem. Phys., 18, 14 511–14 537, https://doi.org/10.5194/acp-18-14511-2018, 2018.

Petit, J.-E., Favez, O., Sciare, J., Crenn, V., Sarda-Estève, R., Bonnaire, N., Močnik, G., Dupont, J.-C., Haeffelin, M., and Leoz-Garziandia, E.: Two years of near real-time chemical composition of submicron aerosols in the region of Paris using an Aerosol Chemical Speciation

Monitor (ACSM) and a multi-wavelength Aethalometer, Atmos. Chem. Phys., 15, 2985–3005, https://doi.org/10.5194/acp-15-2985-2015, 2015.

Pfeifer, S., Müller, T., Weinhold, K., Zikova, N., Martins dos Santos, S., Marinoni, A., Bischof, O. F., Kykal, C., Ries, L., Meinhardt, F., Aalto, P., Mihalopoulos, N., and Wiedensohler, A.: Intercomparison of 15 aerodynamic particle size spectrometers (APS 3321): uncertainties in particle sizing and number size distribution, Atmos. Meas. Tech., 9, 1545–1551, https://doi.org/10.5194/amt-9-1545-2016, 2016.

Schönhardt, A., Altube, P., Gerilowski, K., Krautwurst, S., Hartmann, J., Meier, A. C., Richter, A., and Burrows, J. P.: A wide field-of-view imaging DOAS instrument for two-dimensional trace gas mapping from aircraft, Atmos. Meas. Tech., 8, 5113–5131, https://doi.org/10.5194/amt-8-5113-2015, 2015.

Sluis, W. W., Allaart, M. A. F., Piters, A. J. M., and Gast, L. F. L.: The development of a nitrogen dioxide sonde, Atmos. Meas. Tech., 3, 1753–1762, https://doi.org/10.5194/amt-3-1753-2010, 2010.

Stebel, K., Amigo, A., Thomas, H., and Prata, A.: First estimates of fumarolic SO2 fluxes from Putana volcano, Chile, using an ultraviolet imaging camera, J. Volcanol. Geotherm. Res., 300, 112 – 120, https://doi.org/https://doi.org/10.1016/j.jvolgeores.2014.12.021, 2015.

Wagner, T., Ibrahim, O., Shaiganfar, R., and Platt, U.: Mobile MAX-DOAS observations of tropospheric trace gases, Atmos. Meas. Tech., 3, 129–140, 2010.

Zieger, P., Ruhtz, T., Preusker, R., and Fischer, J.: Dual-aureole and sun spectrometer system for airborne measurements of aerosol optical properties., Applied Optics, 46, 8542–8552, 2007.